# 3D SAP-EPI motion-corrected fast susceptibility weighted imaging

**S. J. Holdsworth[1], S. Skare[1], K. Marty[1], M. Straka[1], and R. Bammer[1]**
[1]Lucas MRS/I Center, Stanford University, Stanford, CA, United States

**Introduction:** Susceptibility-weighted imaging (SWI) has been utilized as a useful contrast mechanism in MRI that accentuates the paramagnetic properties of blood products (1,2). With the use of both magnitude and phase images, SWI can provide improved conspicuity of venous blood vessels and other sources of susceptibility effects (2). Typically, the SWI acquisition uses a high-resolution, three-dimensional gradient echo (GRE) sequence. However, the GRE acquisition used for SWI suffers from a long scan time (~5 mins at 3T), which decreases patient through-put and increases the chances of motion artifacts. A 3D GRE-EPI trajectory has been proposed as a faster alternative. However, unless the data are acquired with several interleaves, the images may suffer from considerable blurring and geometric distortion artifacts. The problem with using multiple interleaves is that, like standard GRE, it makes 3D GRE-EPI vulnerable to motion. Here, a 3D short-axis readout propeller (SAP)-EPI trajectory (3) is suggested as an alternative approach to 3D GRE and 3D GRE-EPI. SAP-EPI can achieve higher resolution than EPI with significantly reduced distortions (4). As a result, fewer interleaves can be used (GRAPPA-acceleration factor $R \leq 4$), making the use of parallel imaging (PI) applicable. With PI, each interleave can be acquired with the full image FOV, making one 'blade' consistent (that is, inter-blade motion is negligible), while the acquisition of one 'brick' can be performed with full brain coverage in a few seconds. The speed of 3D SAP-EPI makes the risk of intra-brick motion (ghosting) small – leaving only the inter-brick 3D motion to be corrected (3). Here we show human 3D SAP-EPI SWI images, as well as demonstrate initial motion-corrected SWI SAP-EPI human data from controlled motion experiments. 3D SAP-EPI is also compared with interleaved 3D EPI as well as with standard 3D GRE.

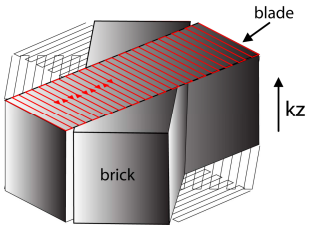


**Fig. 1:** 3D SAP-EPI *k*-space traversal (3). One blade is acquired for every *z*-partition – resulting in one 'brick', which is then rotated. Referenceless Nyquist-ghost calibration parameters (5) are estimated on the middle slice in hybrid-space to correct for each brick, followed by a 1D FFT along $k_z$. GRAPPA weights (6,7) are estimated on each brick (8).

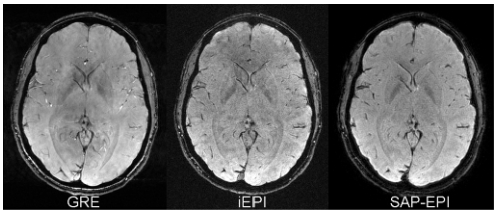


**Fig. 2:** 3D GRE, 3D interleaved EPI (32 shots), and 3D SAP-EPI ($R$ = NEX = 4, 8 blades) original magnitude images.

**Methods:** The 3D SAP-EPI *k*-space trajectory is shown in Fig. 1. Experiments were conducted on a healthy volunteer using a 3T whole-body GE Excite system and an eight-channel head coil. The following scan parameters were used for the SAP-EPI and interleaved EPI sequence: matrix size = 256 x 256, TR/TE/FA = 55ms/20ms/20º, FOV = 24 x 24 x 12.8cm$^3$, 64 *z*-partitions, slthk = 2 mm. The SAP-EPI sequence used 8 blades of width 64, $R$ = NEX = 4, a brick frame rate of 3.5 s, and a scan time of 1:48 min. The EPI sequence used 32 interleaves for an equivalent scan time. Two 3D SAP-EPI datasets were acquired, the second with a through-plane rotation of ~10º. Blade data were mixed, such that every second blade was chosen from the rotated dataset. The $R$ bricks per brick angle originating were 3D motion corrected (in the image domain). All bricks together were then motion corrected prior to gridding (in *k*-space). A high resolution flow-compensated GRE sequence was acquired for comparison (matrix size = 512 x 256, rectangular FOV = 0.75, TR/TE/FA = 37ms/20ms/20º, *z*-partitions = 32, slthk = 2mm, scan time = 5mins). All data were processed by generating a phase mask using a 2D Hanning window. The phase mask was multiplied by the magnitude image 5 times to produce the final SWI image.

**Results:** A comparison between the original magnitude images acquired with 3D GRE, interleaved EPI, and SAP-EPI is shown in Fig. 2. Although the resolution and SNR is highest for the GRE scans, both the interleaved EPI and SAP-EPI scans demonstrate darker vessels in a number of regions. In addition, interleaved EPI and SAP-EPI have a considerably reduced scan time and a better extent of brain coverage (64 partitions in 1:52mins for interleaved EPI and SAP-EPI, versus 32 partitions in 5mins for GRE). Although the scan time of the interleaved EPI scan is equivalent to the SAP-EPI and the vessels are slightly more conspicuous, it has reduced SNR and suffers from ghosting artifacts – even for a cooperative volunteer. Motion artifacts are problematic for both GRE and EPI, as even small patient motion could result in an unusable image. Fig. 3 shows a side-by-side comparison of GRE and SAP-EPI images. While small vessels are more easily depicted in the GRE image, SAP-EPI renders thicker and more prominent larger vessels – probably due to the additional T2*-dephasing that occurs during the EPI readout. Also depicted are motion corrupted SAP-EPI SWI data from the mixed-blade dataset which have been corrected for motion. This example demonstrates an additional advantage of SAP-EPI over GRE and interleaved EPI.

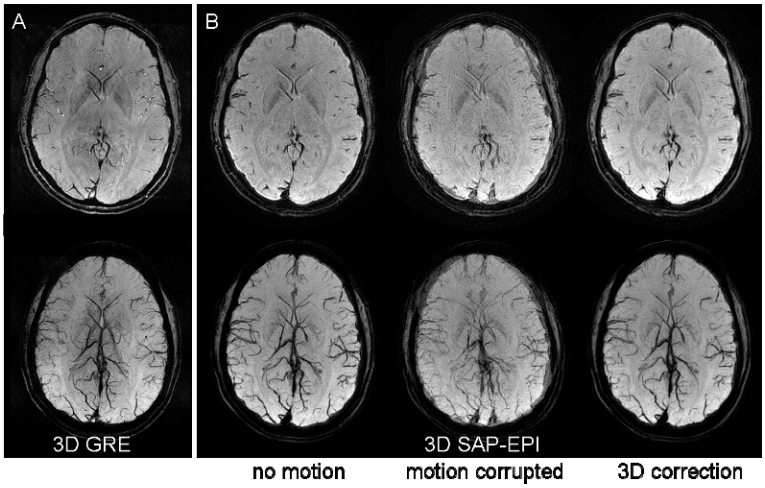


**Fig. 3:** (A) 3D GRE, (B) 3D SAP-EPI SWI (top row) and SWI minIP images (bottom row). Also included in (B) are motionless, motion-corrupted, and 3D motion corrected SAP-EPI images.

**Discussion:** Perhaps one of the greatest hindrances to the adoption of SWI in the clinics is the long scan time associated with standard GRE. However, with parallel imaging, the scan time of GRE can be reduced by up to a factor of 4 (8-channel head coil) – although this can result in a significant SNR penalty. EPI can be used to significantly speed up the acquisition, but with an SNR which makes it more compatible with PI. However, PI-enhanced EPI still suffers from distortion artifacts. On the other hand, multi-shot EPI used *without* PI ($R > 4$), like standard GRE can suffer from severe ghosting in the presence of motion. SAP-EPI helps to alleviate some of these problems. The 'short-axis' blades with a smaller echo-spacing (compared to EPI) result in reduced distortion (roughly proportional to the width of the blade). As a result, fewer interleaves can be used – which enable the use of PI (here R = 4) to give a consistent motion-free blade (that is, a blade acquired at full FOV) in a reduced overall scan time compared with GRE. In addition, any motion that does occur between blades can be corrected for via 3D rigid-body correction. In the event that the brick frame rate (of 3.5 s in this case) results in inter-brick motion, this brick could be re-acquired (3).

**Summary:** Here we have presented SWI images acquired with an efficient propeller-based EPI readout method, which has an inherent ability to allow motion correction. While 3D SAP-EPI still suffers from some geometric distortion, its significantly shorter scan time and relatively high SNR suggest that 3D SAP-EPI may be a useful alternative to GRE for use in susceptibility-weighted imaging, particularly in uncooperative patients.

***References:*** [1] Reichenbach JR et al. Radiology 1997;204:272-77. [2] Hacke EM et al. MRM 2004;52:612-18. [3] Holdsworth SJ et al. ISMRM 2008:1352. [4] Skare S et al. MRM 2006;55:1298-1307. [5] Nordell A et al. ISMRM 2007:1833. [6] Griswold MA et al. MRM 2002;47:1202-1210. [7] Qu P et al. JMR 2005;174(1):60-67. [8] Skare S et al. MRM 2007;57:881–890. **Acknowledgements:** This work was supported in part by the NIH (2R01EB002711, 1R01EB008706, 1R21EB006860), the Center of Advanced MR Technology at Stanford (P41RR09784), Lucas Foundation, Oak Foundation, and the Swedish Research Council (K2007-53P-20322-01-4). We would also like to thank Bronwen Holdsworth for her continuous help.